Origin of high Néel temperature in the low coordination number system $A\mathrm{FeO_2}$ (A=K and Rb)

Minjae Kim, Beom Hyun Kim, Hong Chul Choi, and B. I. Min
Department of Physics, PCTP, Pohang University of Science and Technology, Pohang 790-784, Korea
(Received 5 March 2010; published 10 June 2010)

To explore the origin of high Néel temperature (T_N=930 K) of $\mathrm{KFeO_2}$, which has only 4 coordination number, we have investigated electronic structures and magnetic properties of $A\mathrm{FeO_2}$ (A=K and Rb) by employing the first-principles band-structure method and the Monte Carlo simulation. We have confirmed the observed antiferromagnetic (AFM) ground state of $\mathrm{KFeO_2}$, and obtained nearly identical electronic structures for $\mathrm{KFeO_2}$ and $\mathrm{RbFeO_2}$. We have found that $A\mathrm{FeO_2}$ (A=K and Rb) have the strong covalent-bonding nature between O $2p$ and Fe $3d$ states, which produces the large kinetic superexchange interaction between Fe ions and high T_N. The calculated T_N of $\mathrm{KFeO_2}$ (804 K) is in good agreement with experiment, suggesting that the strong AFM superexchange interaction compensates the low coordination number in $\mathrm{KFeO_2}$. The estimated T_N of $\mathrm{RbFeO_2}$ (821 K) is predicted to be even higher than that of $\mathrm{KFeO_2}$ due to the larger Fe-O-Fe bond angle in $\mathrm{RbFeO_2}$.

DOI: 10.1103/PhysRevB.81.212405 PACS number(s): 75.47.Lx, 75.50.Ee, 71.20.−b

Alkali-metal ferrites $\bar{A}\mathrm{FeO_2}$ ($\bar{A}$: alkali metal) crystallize in diverse structures, depending on $\bar{A}$. For example, lithium ferrite (α-$\mathrm{LiFeO_2}$) has a cubic structure of rocksalt type[1] while sodium ferrite (α-$\mathrm{NaFeO_2}$) has a rhombohedral structure with $R\bar{3}m$ space group.[2] On the other hand, $\mathrm{KFeO_2}$ and $\mathrm{RbFeO_2}$, which are of our present interest, have the orthorhombic $\mathrm{KGaO_2}$-type structures with $Pbca$ space group [Fig. 1(a)].[3] In $\mathrm{KFeO_2}$ and $\mathrm{RbFeO_2}$, $[\mathrm{FeO_4}]^-$ corner-sharing tetrahedra are connected to form the three-dimensional cristobalitelike network [Fig. 1(b)], while K and Rb cations occupy interstices. $\mathrm{CsFeO_2}$, at high temperature, has been known to have a cubic structure with $Fd\bar{3}m$ space group.[3] It is reported only recently that all three $\mathrm{KFeO_2}$, $\mathrm{RbFeO_2}$, and $\mathrm{CsFeO_2}$ have orthorhombic ($Pbca$) structures at low temperature, and upon heating, the structural phase transitions to cubic ($Fd\bar{3}m$) structure take place at 1003 K, 737 K, and 350 K, respectively.[4]

$\mathrm{LiFeO_2}$, $\mathrm{KFeO_2}$, and $\mathrm{RbFeO_2}$ have attracted recent attention due to the possibility of low-cost cathode materials in rechargeable lithium batteries.[5–7] Furthermore, $\mathrm{KFeO_2}$, which has been used as catalyst for dehydrogenation,[8] is known to have the highest Néel temperature (T_N=930 K) among iron oxides.[9] T_N of $\mathrm{KFeO_2}$ having only 4 nearest-neighbor (NN) coordination number is much higher than that of $\mathrm{LaFeO_3}$ (T_N=750 K) having 6 NN coordination.[10] Note that T_N is proportional to the number of the NN coordination. Then the high T_N of $\mathrm{KFeO_2}$ implies that there exists strong antiferromagnetic (AFM) exchange interaction which compensates its low coordination number. Shorter Fe-O bond lengths in $\mathrm{KFeO_2}$ (1.79–1.93 Å) than those in $\mathrm{LaFeO_3}$ (~2.00 Å) hints at the stronger kinetic superexchange interaction in $\mathrm{KFeO_2}$ than in $\mathrm{LaFeO_3}$. However, electronic and magnetic properties of $\mathrm{KFeO_2}$ in relation to its characteristic crystal structure have not been explored yet.

$\mathrm{RbFeO_2}$ is isostructural to $\mathrm{KFeO_2}$. The Fe-O bond lengths of $\mathrm{RbFeO_2}$ (1.85–1.87 Å) are similar to those of $\mathrm{KFeO_2}$ but the Fe-O-Fe bond angles are different between two. Due to larger ionic size of $\mathrm{Rb^+}$ than $\mathrm{K^+}$, the Fe-O-Fe bond angle is larger for $\mathrm{RbFeO_2}$ (~144°) than for $\mathrm{KFeO_2}$ (~135°).[3] According to the Goodenough-Kanamori-Anderson rule,[11] the larger Fe-O-Fe bond angle would produce the larger AFM superexchange interaction. Accordingly, it is expected that $\mathrm{RbFeO_2}$ would have higher T_N than $\mathrm{KFeO_2}$. However, such possibility has not been tested experimentally or even theoretically yet.

In this Brief Report, we have investigated electronic structures and magnetic properties of $A\mathrm{FeO_2}$ (A=K and Rb) using the first-principles electronic-structure method and the Monte Carlo (MC) simulation. We have found that $A\mathrm{FeO_2}$ (A=K and Rb) have strongly hybridized O $2p$ and Fe $3d$ states which look like molecular bond states. These localized states are responsible to induce the strong kinetic superexchange interaction between NN Fe ions, resulting in such high T_N for low coordination number system: $A\mathrm{FeO_2}$ (A=K and Rb).

We have performed total-energy band-structure calculations employing the full-potential augmented plane-wave band method[12] which is implemented in WIEN2K package.[13] We have used the generalized gradient approximation (GGA) of the PBE96 form for the exchange-correlation potential.[14] The valence wave functions inside the muffin-tin spheres are

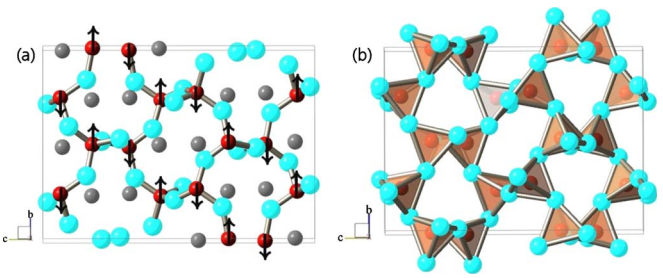

FIG. 1. (Color online) (a) Orthorhombic crystal structure of $\mathrm{KFeO_2}$. K, Fe, and O are represented by medium (gray), dark (red), and light (cyan) spheres, respectively. In the AFM ground state of $\mathrm{KFeO_2}$, all the NN Fe ions are coupled antiferromagnetically to each other. ↑ and ↓ at Fe ions denote the spin directions. $\mathrm{RbFeO_2}$ has a structure similar to $\mathrm{KFeO_2}$ but with larger Fe-O-Fe bond angles. (b) The Cristobalite ($\mathrm{SiO_2}$)-like network formed with $[\mathrm{FeO_4}]$ corner-sharing tetrahedra in $A\mathrm{FeO_2}$.

TABLE I. Total-energy difference between the FM and the AFM state of $KFeO_2$ and $RbFeO_2$, and the magnetic moment $M_{calc.}$ of Fe obtained in our band-structure calculations. The experimental magnetic moment $M_{expt.}$ of Fe in $KFeO_2$ is also given for comparison (Ref. 9). No experimental value is available for $RbFeO_2$.

	$E_{FM}-E_{AFM}$ (eV/f.u.)	$M_{calc.}$ (μ_B)	$M_{expt.}$ (μ_B)
$KFeO_2$	0.701	3.44	4.00
$RbFeO_2$	0.716	3.43	···

expanded with spherical harmonics up to $l_{max}=10$. The wave function in the interstitial region is expanded with plane waves up to $K_{max}=5.5/R_{MT}$, where R_{MT} is the smallest muffin-tin sphere radius. R_{MT} were set as 2.35 a.u. for K and Rb, 2.00 a.u. for Fe, and 1.35 a.u. for oxygen. The charge density was expanded with plane waves up to $G_{max}=12$ $(a.u.)^{-1}$. We have used 100 k points inside the first Brillouin zone. The convergence of the total energy with respect to number of k points was checked to have precision of less than 0.1 meV per formula unit (f.u.).

Structural parameters for both $KFeO_2$ and $RbFeO_2$ were employed from experiment.[15,3] As shown in Fig. 1, both $KFeO_2$ and $RbFeO_2$ have the orthorhombic structure with AFM ground state. All the NN Fe ions are coupled antiferromagnetically. Lattice constants for $KFeO_2$ are $a=5.594$ Å, $b=11.247$ Å, and $c=15.863$ Å, and those for $RbFeO_2$ are $a=5.757$ Å, $b=11.514$ Å, and $c=16.283$ Å. There are two independent atomic types for A (A=K and Rb) and Fe, while four independent atomic types for oxygen.

To evaluate T_N, we have performed the MC simulation for a $24\times6\times6$ supercell with periodic boundary condition. Based on the total-energy band-structure results, we have derived the classical spin Hamiltonian considering only the NN exchange interaction between Fe ions,

$$H = H_0 + J\sum_{\langle i,j\rangle} \vec{S}_i \cdot \vec{S}_j. \quad (1)$$

Here H_0 is the spin-independent Hamiltonian, J is the exchange constant between NN Fe ions, which can be estimated from the total-energy difference between the ferromagnetic (FM) and the AFM state, and S is the magnetic moment of Fe ion obtained in our band-structure calculation, as provided in Table I. By using the Wolff's cluster algorithm,[16] we have spanned 18 000 thermalization and 36 000 calculation steps at each temperature to calculate physical quantities in the MC simulation. T_N was determined by the peak position of the magnetic susceptibility.

Table I presents the total-energy differences between the FM and the AFM state of $AFeO_2$ (A=K and Rb). We have obtained more stable AFM ground state for $KFeO_2$ as is consistent with experiment. We have obtained the stable AFM ground state for $RbFeO_2$ too. Mössbauer experiment[15] for $KFeO_2$ indicated that both Fe ions at two independent positions exist in the ferric trivalent (Fe^{3+}:d^5) state with the high-spin configuration. But the magnetic moment of Fe^{3+} ion is observed to be much reduced from ideal $5.0\mu_B$ to

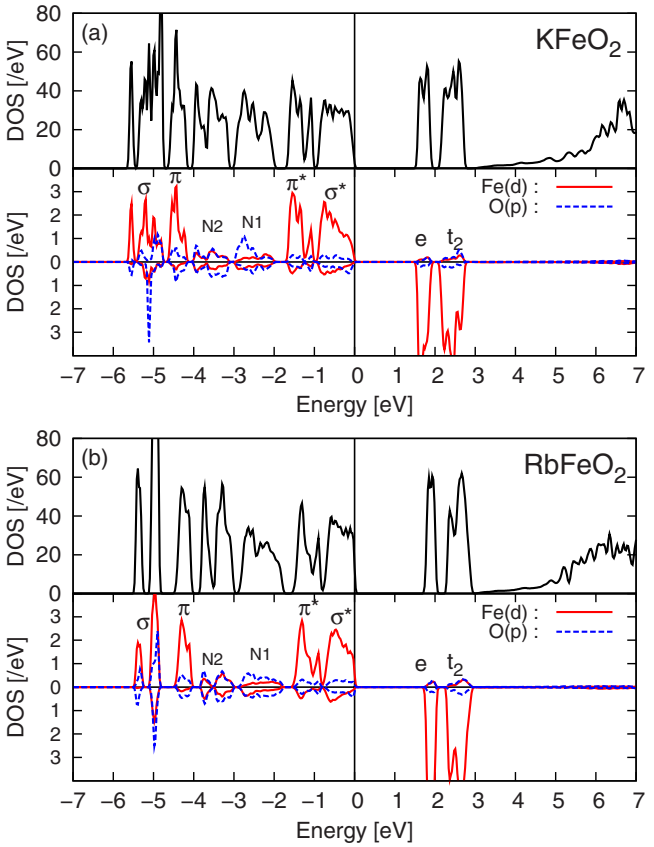

FIG. 2. (Color online) (a) Total and partial DOS for the AFM phase of $KFeO_2$. Fe d and O p partial DOS are represented by solid (red) and dashed (blue) lines, respectively, in the lower panel. The p-d bonding (σ,π), antibonding (π^*,σ^*), and nonbonding (N1, N2) states in the majority spin and unoccupied e and t_2 states in the minority spin are identified in the lower panel. (b) The same as the above for $RbFeO_2$.

$\sim 4.0\mu_B$ because of strong covalency effect with neighboring oxygen ions.[9] Our band calculation for $KFeO_2$ reveals that Fe ions at two independent positions of $KFeO_2$ have almost identical electronic states and magnetic moments. The calculated magnetic moment of $3.44\mu_B$ in Table I also supports the strong covalency effect between Fe and oxygen. Fe ions in $RbFeO_2$ are also in the ferric state and have the magnetic moment of $3.43\mu_B$, which is close to that in $KFeO_2$.

Figure 2 shows the density of states (DOS) of $AFeO_2$ (A=K and Rb) in their AFM ground states. Note that electronic structures of $KFeO_2$ and $RbFeO_2$ are similar to each other. Both have insulating band structures with nearly trivalent Fe^{3+} states with high-spin configurations. The size of band gap is 1.50 eV for $KFeO_2$ and 1.70 eV for $RbFeO_2$. The occupied valence states are composed of molecular bondlike states formed with O $2p$ and Fe $3d$ states. The s and p states of the alkali-metal ions (K and Rb) are far above the unoccupied Fe $3d$ states, and so have no important effects on the valence-band structure. Due to the tetrahedral crystal field from surrounding oxygens, t_2 states of Fe will be located above e states in energy. Then t_2 states will be hybridized with O $2p$ states through σ channel while e states through π channel. Due to short Fe-O bond lengths in $AFeO_2$, the hy-

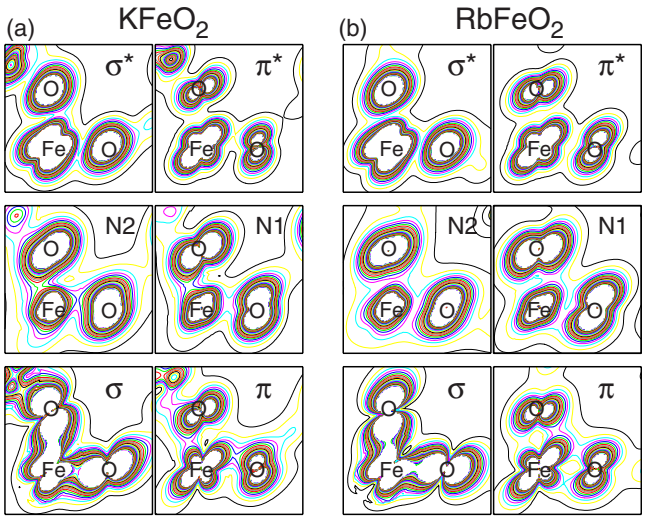

FIG. 3. (Color online) (a) Charge densities of σ, π, N2, N1, π^*, and σ^* states for $KFeO_2$. Planes are chosen to contain O-Fe-O atoms. (b) The same as the left for $RbFeO_2$.

bridization in the σ channel is much stronger than that in the π channel. As a result, σ is located below π in the bonding states while σ^* is located above π^* in the antibonding states, so as to have σ, π, π^*, and σ^* order, as manifested in Fig. 2 (see the majority-spin states). This feature will be demonstrated below in Fig. 3. In contrast, in the minority-spin states, there is almost vanishing hybridization between Fe $3d$ and O $2p$ states to show bare e and t_2 states. The N1 and N2 correspond to nonbonding states originating mostly from O $2p$ states. We have checked that the essential feature of the GGA electronic structure for $AFeO_2$ (A=K and Rb) is preserved also in the GGA+U (U: on-site Coulomb interaction) scheme for $U=1-5$ eV.[17]

In Fig. 3 are plotted the charge densities of molecular bondlike σ, π, π^*, and σ^* states and nonboding N1 and N2 states, which are identified in Fig. 2. Charge densities of $KFeO_2$ and $RbFeO_2$ are similar to each other. The charge densities in the σ and σ^* states are directed toward oxygen ions demonstrating their t_2 origin while those in the π and π^* states are directed in between oxygen ions demonstrating their e origin. Nonbonding states N1 and N2 have small contribution also from Fe $3d$ states, and thereby they are split by having slightly σ character for N2 and π character for N1. Most prominent is that the σ bonding is nearly covalent and much stronger than the π bonding. This strong covalent bonding nature in $AFeO_2$ is expected to produce the large kinetic superexchange interaction between Fe ions to give rise to high T_N.

Figure 4 provides the band structures of $AFeO_2$ (A=K and Rb). Bands with larger Fe $3d$ components are plotted with larger red dots (left) while those with larger O $2p$ components with larger blue dots (right). Band structures of $KFeO_2$ and $RbFeO_2$ are similar to each other. Nearly flat bands with thicker red color correspond to highly localized bonding and antibonding states of σ, π, π^*, and σ^*. On the other hand, dominant O $2p$ components with thicker blue color are apparent for bonding σ and nonbonding N2, N1 states. It is clearly seen that the contribution of Fe $3d$ components is minor for N2 and N1 states.

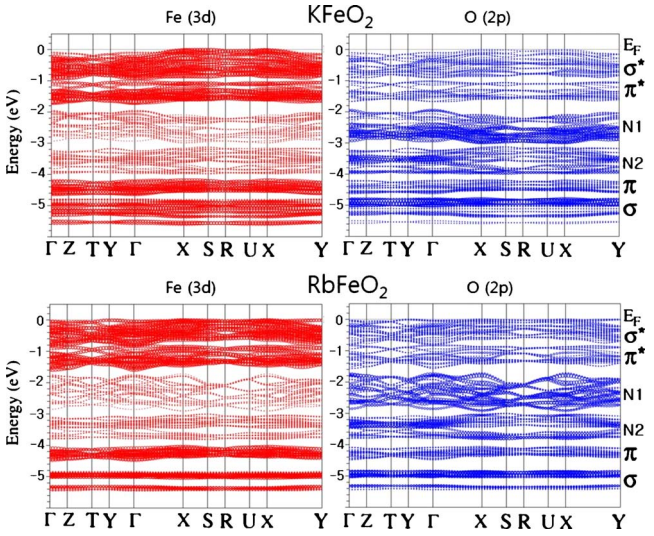

FIG. 4. (Color online) (Top) Band structure of $KFeO_2$. The size of red (blue) dot denotes the amount of Fe $3d$ (O $2p$) component in the wave function. (Bottom) The same as the above for $RbFeO_2$.

We have evaluated the Néel temperature T_N of $AFeO_2$ (A=K and Rb) employing the MC simulation. We have considered only the NN exchange interaction in Eq. (1). The hopping interaction between next-nearest-neighbor (NNN) Fe ions should be small due to the full occupancy of the majority-spin Fe d states in the AFM ground state of $AFeO_2$. Further, the low coordination number, 4, with cristobalitelike network, reduces the hopping interaction between NNN Fe ions due to small number of channels. In fact, there is only one channel having shortest distance between NNN Fe ions. Also $T^{3/2}$ dependence of the magnetic hyperfine field observed in Mössbaouer experiment[15] supports the dominance of the NN exchange interaction, which induces the long-wavelength spin waves excitation. Therefore, the hopping interaction between NN Fe ions will play an essential role in magnetism of $AFeO_2$ (A=K and Rb).

Table II presents the estimated exchange constant J from the total-energy band-structure results and resulting T_N for $AFeO_2$ (A=K and Rb) obtained from the MC simulation. Interestingly, the calculated T_N=804 K for $KFeO_2$ is in fairly good agreement with experimental T_N=930 K. This agreement reflects that high T_N in $KFeO_2$ results really from the strong AFM kinetic superexchange interaction between NN Fe ions. The estimated J of $RbFeO_2$ is 7.60 meV, which is even larger than that of $KFeO_2$ (7.40 meV). The stronger superexchange interaction in $RbFeO_2$ is attributed to a larger

TABLE II. Evaluated Néel temperature T_N's of $KFeO_2$ and $RbFeO_2$ from the MC simulation. The exchange constant J is estimated from the total-energy difference in Table I. The experimental value of T_N for $KFeO_2$ is also given for comparison (Ref. 15).

	J (meV)	T_N (calc.) (K)	T_N (expt.)
$KFeO_2$	7.40	804	930 K
$RbFeO_2$	7.60	821	···

Fe-O-Fe bond angle of $RbFeO_2$,[3] which induces stronger AFM exchange interaction. Therefore, calculated T_N of $RbFeO_2$ (821 K) is higher than that of $KFeO_2$ (804 K). This predicted higher T_N in $RbFeO_2$ needs to be tested experimentally.

We mentioned above that perovskite $LaFeO_3$ has lower T_N (750 K) than $KFeO_2$, despite the higher coordination number. According to band results[18,19] for $LaFeO_3$, Fe ions exist in the high-spin configuration with the magnetic moment of $4.06\mu_B$, and the energy difference between the FM and the G-type AFM state is 0.318 (eV/f.u.). Then the exchange constant J is estimated to be 1.61 meV, which is five times smaller than J of $KFeO_2$ (7.40 meV). This difference in J is due to the different Fe-O bond lengths between two structures. Due to much longer Fe-O bond length in $LaFeO_3$, the hopping interaction and the associated p-d hybridization are not so strong as in $KFeO_2$. Much weaker p-d hybridization in $LaFeO_3$ is revealed in its electronic structure. Fe $3d$ states in $LaFeO_3$ are composed of bare t_{2g} and e_g states arising from the octahedral crystal field of surrounding oxygens,[18] contrary to the molecular bondlike state of σ, π, π^*, and σ^* in $KFeO_2$.

We have investigated electronic structures and magnetic properties of $AFeO_2$ (A=K and Rb). We have confirmed the observed insulating and AFM ground state for $KFeO_2$. Electronic and magnetic properties of $RbFeO_2$ are almost identical to those of $KFeO_2$. The strong p-d hybridization originating from short Fe-O lengths in $AFeO_2$ (A=K and Rb) produces molecular bondlike states, σ, π, π^*, and σ^*, in the occupied majority-spin states. Such highly localized states yield the strong kinetic superexchange interactions between the Fe ions and high T_N in $AFeO_2$ (A=K and Rb). The calculated T_N of $KFeO_2$ based on the estimated NN exchange interaction is in good agreement with experiment. The calculated T_N of $RbFeO_2$ is higher than that of $KFeO_2$, which predicts that $RbFeO_2$ rather than $KFeO_2$ would be the highest T_N material among Fe oxides.

This work was supported by the NRF (Grant No. 2009-0079947) and by the steel science project of POSCO.

[1] E. Posnjak and T. F. W. Barth, Phys. Rev. **38**, 2234 (1931).
[2] T. McQueen, Q. Huang, J. W. Lynn, R. F. Berger, T. Klimczuk, B. G. Ueland, P. Schiffer, and R. J. Cava, Phys. Rev. B **76**, 024420 (2007).
[3] J. Nuss, N. Z. Ali, and M. Jansen, Acta Crystallogr., Sect. B: Struct. Sci. **63**, 719 (2007).
[4] N. Z. Ali, J. Nuss, D. Sheptyakov, and M. Jansen, J. Solid State Chem. **183**, 752 (2010).
[5] K. Edström, S. Ito, and R. G. Delaplane, J. Magn. Magn. Mater. **212**, 347 (2000).
[6] M. Tabuchi, K. Ado, H. Sakaebe, and C. Masquelier, Solid State Ionics **79**, 220 (1995).
[7] S. J. Moon, S. J. Kim, and C. S. Kim, J. Korean Phys. Soc. **52**, 406 (2008).
[8] A. Kotarba, A. Barański, S. Hodorowicz, J. Sokołowski, A. Szytuła, and L. Holmlid, Catal. Lett. **67**, 129 (2000).
[9] Z. Tomkowicz and A. Szytua, J. Phys. Chem. Solids **38**, 1117 (1977).
[10] U. Shimony and J. M. Knudsen, Phys. Rev. **144**, 361 (1966).
[11] J. B. Goodenough, *Magnetism and the Chemical Bond* (Interscience, New York, 1963).
[12] M. Weinert, E. Wimmer, and A. J. Freeman, Phys. Rev. B **26**, 4571 (1982); S.-W. Seo, Y. Y. Song, G. Rahman, I. G. Kim, M. Weinert, and A. J. Freeman, J. Magn. **14**, 137 (2009).
[13] P. Blaha, K. Schwarz, G. K. H. Madsen, D. Kavasnicka, and J. Luitz, in *WIEN2k*, edited by K. Schwarz (Technische Universitat Wien, Austria, 2001).
[14] J. P. Perdew, K. Burke, and M. Ernzerhof, Phys. Rev. Lett. **77**, 3865 (1996).
[15] S. J. Moon, I.-B. Shim, and C. S. Kim, IEEE Trans. Magn. **42**, 2879 (2006).
[16] U. Wolff, Phys. Rev. Lett. **62**, 361 (1989).
[17] V. I. Anisimov, I. V. Solovyev, M. A. Korotin, M. T. Czyzyk, and G. A. Sawatzky, Phys. Rev. B **48**, 16929 (1993).
[18] Z. Yang, Z. Huang, L. Ye, and X. Xie, Phys. Rev. B **60**, 15674 (1999).
[19] I. R. Shein, K. I. Shein, V. L. Kozhevnikov, and A. L. Ivanovskiĭ, Phys. Solid State **47**, 2082 (2005).